Construction and Building Materials 259 (2020) 119679

Contents lists available at ScienceDirect

Construction and Building Materials

journal homepage: www.elsevier.com/locate/conbuildmat

Fracture properties of reclaimed asphalt pavement mixtures with rejuvenator

J.K. Ong [a], L. Gungat [b,*], M.O. Hamzah [c]

[a] Samwoh Innovation Centre, Samwoh Corporation, Singapore 728661, Republic of Singapore
[b] Civil Engineering Program, Faculty of Engineering, Universiti Malaysia Sabah, 88400 Kota Kinabalu Sabah, Malaysia
[c] School of Civil Engineering, Engineering Campus, Universiti Sains Malaysia, 14300 Nibong Tebal, Seberang Perai Selatan, Penang, Malaysia

HIGHLIGHTS

- High variability of RAP sources and potential of crack distress when using high RAP remain an inherent concern for RAP.
- Needs to study the fracture properties of RAP mixtures at a micro-level.
- Employed conventional and innovative approach to evaluate the fracture characteristics of high RAP mixture.
- The fractured surfaces were quantified using geospatial imaging technique.

GRAPHICAL ABSTRACT

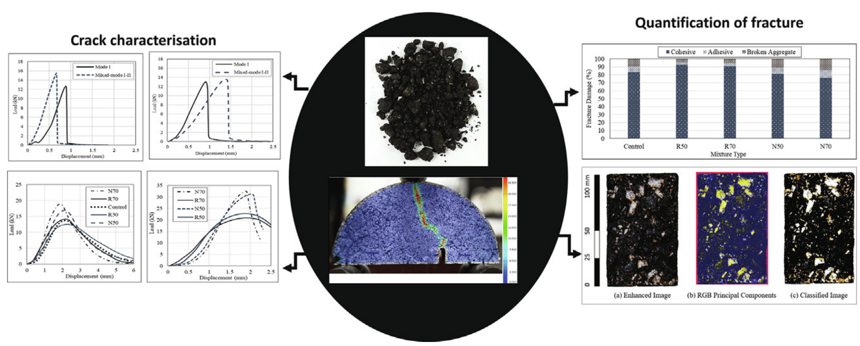

ARTICLE INFO

Article history:
Received 24 December 2019
Received in revised form 24 May 2020
Accepted 25 May 2020
Available online 22 June 2020

Keywords:
Reclaimed asphalt pavement
Rejuvenator
Geospatial imaging technique
Fracture properties

ABSTRACT

Reclaimed asphalt pavement (RAP) technology has been extensively promoted to conserve depleting virgin materials for asphalt mixtures. High RAP content is desirable from economic and environmental standpoints. However, RAP mixtures become too stiff and require modification such as rejuvenator. This paper presents the evaluation on the fracture characteristics of mixtures prepared with 50% and 70% RAP, with and without rejuvenator that were subjected to indirect tensile strength (ITS) and notched semi-circular bending (SCB) tests. The fractured surfaces of the tested specimens were quantified using geospatial imaging technique to identify the proportion contribution to failure, namely cohesive, adhesive and broken aggregates. The results showed that the fractured rejuvenated mixtures were predominantly of the cohesive type when compared with the non-rejuvenated mixtures. On the other hand, the failure modes of non-rejuvenated mixtures were of the adhesive and aggregate failure types. The measured ITS at two temperatures corresponded with the expected damage trends. Similar behaviour was found in the derived fracture energy and pre-peak slope that were obtained from the SCB pure tensile and tensile-shear load–displacement curves. The findings showed that the fracture properties of rejuvenated mixtures performed comparably with virgin mixtures in terms of fracture toughness, tensile strength and proportion of damage contribution.

1. Introduction

The mounting task of maintaining an extensive and rapidly ageing road networks has shifted paving towards concepts that value reusability and sustainability. While low RAP content up to 30% has

* Corresponding author.
E-mail address: lillian@ums.edu.my (L. Gungat).

https://doi.org/10.1016/j.conbuildmat.2020.119679

been adopted comfortably in road construction, the feasibility of high RAP application continues to be questioned [1]. Such concern is attributed to the variability of RAP mixture performance, especially when a very high RAP content or a new rejuvenator is used [2].

Despite the known limitations, 100% RAP usage in road construction has long been achieved in the Netherlands and Denmark [3]. Hansen and Copeland [4] reported in a nationwide survey that more than 99% of RAP material was reused in new pavements, while other European countries reported a very high use of RAP in hot and warm asphalt productions [5]. RAP technology is highly sought-after for a number of reasons. For instance, Zaumanis et al. [2] reported $20 per ton cost savings when 50% RAP content mixture was used as an alternative. The life cycle assessment of pavement also showed that a low recycling rate of 15% brought significantly lower environmental impacts than warm mix asphalt (WMA) [6]. Other benefits also include energy conservations, resource preservation and waste reduction [1]. No doubt, the benefits of RAP technology outweigh the cost from both environmental and economic standpoints. This has driven continuous innovations for a more efficient RAP mixture constituting different RAP contents and rejuvenators. It is well-established that RAP mixture is susceptible to crack distresses and potentially ravelling [7–8]. This is particularly true when a full binder activation is not achieved through high temperature or sufficient rejuvenation [8–9]. The RAP aggregate stays functionally as a 'black rock' in theory when virgin materials adhere on the surface of a fully coated RAP aggregate [10]. A field survey suggested that RAP aggregates can either be partially or fully coated with aged binder in reality before mixing with virgin materials [11]. Thus, the composite behaviours of RAP-virgin mixture in resisting pavement distresses remain debatable. This presents a need to study the fracture properties of RAP mixtures at a micro-level.

Over the years, limited headway was made to quantify the failure modes of fractured specimens from a visual approach. In other words, evaluation based on human vision is often subjective due to the inherent differences of human perception towards lights and colours. Recent studies highlighted the use of a digital imaging technique to evaluate the moisture susceptibility and fracture properties of WMA [12–14]. This technique quantifies the fractured surfaces digitally into three distinct failure modes, namely cohesive, adhesive and broken aggregates. Although this technique was widely applied to investigate fracture behaviours of WMA, similar studies on RAP mixtures are rather limited. Previous research suggested that insufficient rejuvenation in RAP mixtures may also result in poor adhesion and cohesion in the mixture [8]. In asphalt technology, the notched SCB test was used to determine the fracture toughness of the asphalt mixtures resulting from pure tensile and tensile-shear fractures. When the pavement is subjected to a moving wheel load and thermal stresses, tensile-shear induced fracture is more likely to occur [15–16]. The fracture energy and stiffness can be computed from the load–displacement curves of a mixture specimen.

Till now, the high variability of RAP sources and the development of new rejuvenators remain an inherent concern for RAP technology. A rejuvenator that had certain effects on one RAP source may not necessarily result in the same effects on another RAP source [17]. Hence, this paper aims to employ conventional and innovative approach to evaluate the fracture characteristics of RAP mixture incorporating different RAP contents, with and without rejuvenator that were subjected to ITS and notched SCB tests. Two SCB configurations are used in this paper and geospatial imaging technique allowed the aforementioned fractures to be simulated.

2. Methodology

2.1. Materials and sample preparation

Raw materials used in this study included RAP, granite aggregate, PG-64 base binder, filler and rejuvenator. The granite aggregates were sourced from Kubang Semang Quarry, Penang, while the RAP aggregates were milled from the North-South Expressway (NSE) which is an interstate toll highway. These aggregates were apportioned according to the Malaysian Public Works Department (PWD) [18] mix type Asphaltic Concrete 14 (AC14) whose gradation is shown in Table 1. The AC 14 gradation is equivalent to nominal maximum aggregate size (NMAS) 12.5 in superpave gradation.

Virgin PG-64 binder supplied by Shell Sdn. Bhd. was used concurrently with the existing RAP binder from the milled aggregates. Properties of the recovered binder was determined by Gungat (2016) [19] in an earlier study. The penetration and softening point of the RAP recovered binder are 19 dmm and 71 °C, respectively. Table 2 presents the penetration of RAP recovered binder blended with different dosages of rejuvenator [20].

Pavement modifier (PMD) was the filler material used. It also acted as an anti-stripping agent. A commercial rejuvenator which commonly used for hot recycling allows coherent mixing of an asphalt mixture with very high recycling content (60% – 100%). The rejuvenator behaves like a viscous liquid and is an oil free rejuvenator synthesised from 100% natural resins. By imposing steric hindrance, the resins would neutralise polarised asphaltenes and restore the original SARA composition of binder [20]. Fig. 1 illustrates the rejuvenator used.

The mix design followed closely methods developed by Hamzah [21]. For ease of reference, mixtures are designated as shown in Table 3.

As mentioned earlier, sufficient rejuvenation is vital to optimise mixture performance. The technical report suggests that only a small difference in dosage suffice to rejuvenate R50 and R70 mixtures as shown in Table 4. Thick and viscous behaviour of the rejuvenator was difficult to handle as the residue may adhere to any typical laboratory container during dissemination, resulting in mixed mixture performance. Thus, a syringe was used to apply the rejuvenator directly on the RAP aggregate during mixing.

Another crucial component in specimen preparation is the mixing sequence. Fig. 2 comprehensively summarises the flow of the mixing sequences for each mixture group. Some of the best practices applied in this study were inspired by mixing technique outlined by previous studies [10,21,22].

2.2. Experimental procedures

2.2.1. Indirect tensile test

The Indirect Tensile Test (ITS) samples were tested at 15 °C and 25 °C according to ASTM D6931-17 [23] procedures. All 100 mm cylindrical specimens were preconditioned for 4 h prior to testing under uniaxial loading at the rate of 50.8 mm/min until failure.

2.2.2. Semi-Circular bending test

The Semi-Circular Bending Test (SCB) samples with 150 mm diameter were divided equally at the centre into two and preconditioned at 10 °C for 4 h prior to the test with reference to AASHTO TP 124 [24] guidelines. For the mixed-mode I/II, a modified SCB test was carried out using an offset notch as proposed by Ameri et al. [25]. The configurations are summarised in Table 5 and illustrated in Fig. 3.

The computations assumed fracture energy, W_f to be equivalent to the full area under the load–displacement curve as shown in the

Table 1
Aggregate gradation.

Sieve Size (mm)	20	14	10	5	3.35	1.18	0.425	0.15	0.075
Limits	100	90–100	76–86	50–62	40–54	18–34	12–24	6–14	4–8
Passing (%)	100	90	76	50	40	18	12	8	6

Table 2
Binder penetration (Van Weezenbeek Specialties, 2017).

Binder Type	Control	Aged Binder	Rejuvenated Binder, 5%	Rejuvenated Binder, 10%
Penetration at 25 °C (dmm)	66	19	39	73

Fig. 1. Commercial rejuvenator.

Table 3
Mixture designation.

RAP (%)	Mortar State	Mixture Designation	Group Designation
0	Virgin	Control	Virgin mixtures
50	Rejuvenated	R50	Rejuvenated mixtures
70	Rejuvenated	R70	Rejuvenated mixtures
50	Not rejuvenated	N50	Non-rejuvenated mixtures
70	Not rejuvenated	N70	Non-rejuvenated mixtures

Table 4
Approximate rejuvenator dosage required in asphalt mixtures.

Required Rejuvenator	R50 (g)	R70 (g)	Difference (g)
Approximate dosage per kg mixture	3.0–4.0	4.0–6.0	1.0–2.0

shaded region of Fig. 4 and calculated using Equation (1). The pre-peak slope is computed from 4 and 8 kN load increment to determine the flexibility.

$$G_f = g\frac{W_f}{A_{lig}} \quad (1)$$

where G_f is the fracture energy (J/m^2), W_f is the integral of P *du*, P is the applied load (N), u is the average load-line displacement (m) and A_{lig} is the ligament area (m^2).

2.2.3. Imaging technique

The fractured surfaces of ITS and SCB test specimens were further examined for quantification of surface fracture by employing two-dimensional Geospatial Imaging Technique. A geospatial software named ArcGIS 10.4 was used to digitalise, classify and quantify the surface features of a fractured mixture. Fig. 5 describes the flow of the geospatial imaging technique used.

The image transformation process using supervised classification of RGB principal components is illustrated in Fig. 6(a), 6(b) and 6(c). Identifying the RGB principal components required the use of the spatial analyst extension in ArcGIS 10.4. After the RGB imagery was created, at least eight training samples were made for each damage type to categorise cohesive, adhesive and broken aggregate surfaces from the enhanced image. These samples were known as region of interest (ROI). Under human supervision, the software was guided to classify the processed RGB images according to the ROI. Then, the supervised classification output was compared with the original specimen surface. Any misclassified region was rectified. The final procedure involved the use of classify raster tool. Image classification was performed and the surface damages were categorised into the three damage types. Corresponding colours were subsequently assigned as illustrated in Fig. 6(c) where black, yellowish-brown and white pixels were identified as cohesive, adhesive and aggregate damages, respectively. The number of pixels for each damage type was then quantified and compared.

3. Results and discussion

3.1. Indirect tensile strength

The ITS test results are shown in Fig. 7, while Table 6 presents the ITS statistical classification resulted from Tukey's range test. From the Tukey's range test, mixture types which do not share a common alphabet such as group A, group B and group C are significantly different in means. For instance, Table 6 shows that N50 and N70 mixtures shared similar ITS when tested at 15℃, therefore they are grouped under a common alphabet, C. Similar description is applied to all Tukey's range test in this paper.

Interestingly, the ITS trends resulted from two different temperatures do not correspond, instead two different trends were observed for each test temperature. An ascending ITS trend was observed when the mixtures were evaluated at 25℃, corresponding with an increase in RAP content. The ITS decreased when RAP content increased at a lower test temperature for rejuvenated and non-rejuvenated mixtures. Furthermore, the rejuvenation effects were found to be significant at both temperatures as the rejuvenated mixtures performed comparably with the virgin mixture as indicated in Table 6.

Temperature governs the mortar stiffness which in turn influences the asphalt mixture's fracture potential. In the ITS test, mixtures experienced deformation prior to rupture when acted upon by an applied load loaded at the two test temperatures. Under this condition, it can be observed that the influence of mortar stiffness outweighed the aggregate strength when rupture took place. Therefore, mixtures with stiffer mortar like N70 experienced a

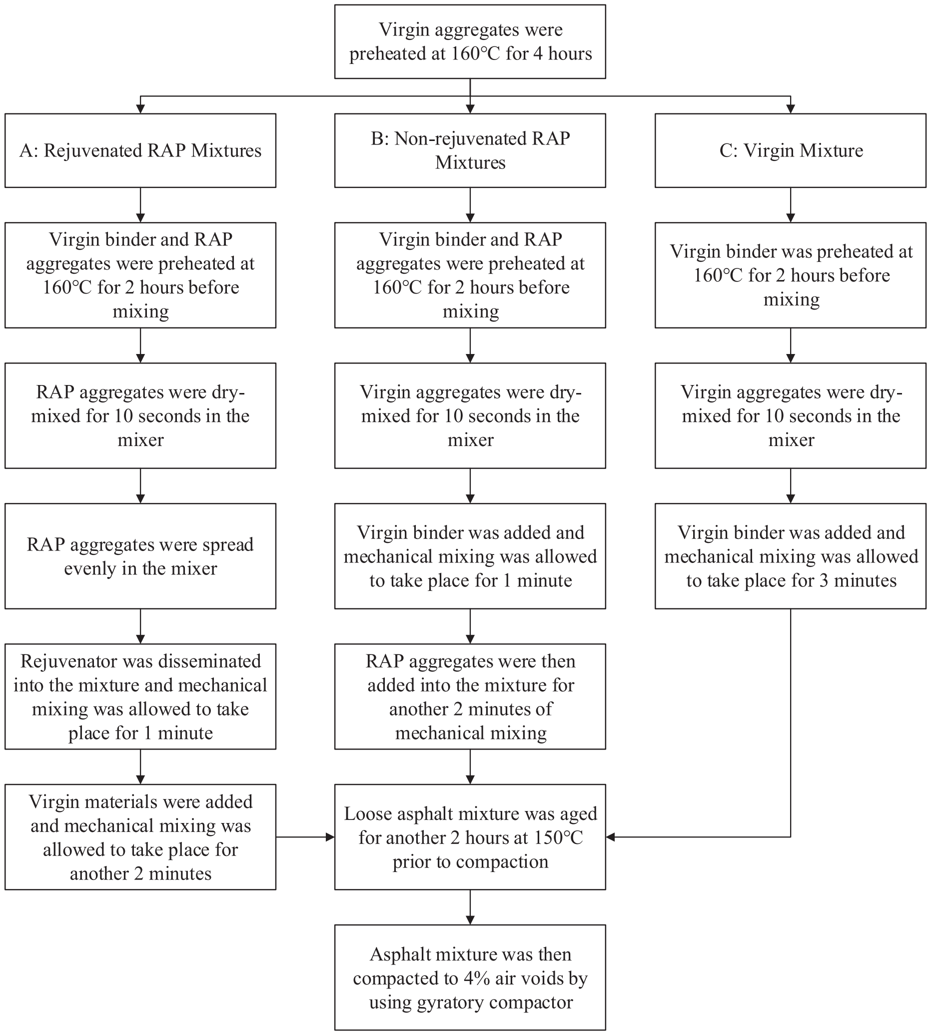

Fig. 2. Flowchart of asphalt mixing procedures.

Table 5
Test parameters for notched SCB test.

Parameter	Mode I	Mixed-mode I/II
Radius, R (mm)	75	75
Notch length, a (mm)	15	15
Notch width (mm)	5	5
Crack ratio, a/R	0.2	0.2
Offset, L (mm)	0	20.4
L/R	0	0.272
2S (mm)	120	120
Loading rate (mm/min)	50.8	50.8
Test temperature (°C)	10	10

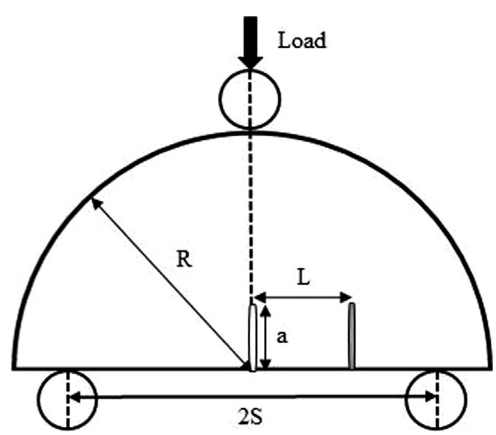

Fig. 3. Notched SCB test loading configurations for pure tensile and tensile-shear fractures.

delayed rupture resulting in higher ITS than N50 at 25℃. When compared, a similar scenario was also observed between R70 and R50 mixtures, as well as between rejuvenated and non-rejuvenated mixtures. At warm temperature, the mixture rupture was highly stiffness-dependent. In relative terms, the fracture potential was slightly less stiffness-dependent at a lower temperature as the dissimilarity in mortar stiffness is smaller. Hence, aggregate strength would have a bigger role in resisting fracture. Fig. 8 describes the typical load–displacement curves at 15℃ and 25℃.

Compensated with higher proportion of virgin aggregates, these mixtures would result in higher ITS as fracture tends to split an aggregate rather than bypassing it. Findings by Sun et al. [15] suggested that at lower temperature, cracks would fracture through aggregates, while at a higher temperature, it would bypass the aggregates and result in smaller proportion of failed contacts occurring in aggregates. Moreover, the author found that at low temperature, fracture energy of the mixtures was in agreement with the number of failed contacts and crack morphology. These

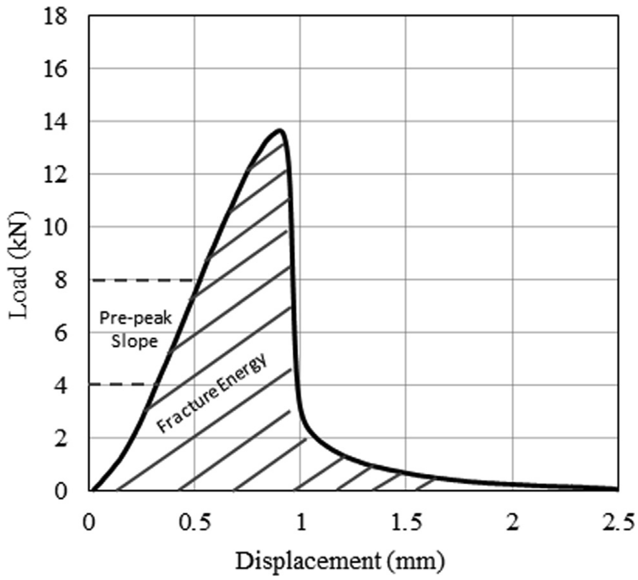

Fig. 4. Calculation of pre-peak slope and fracture energy.

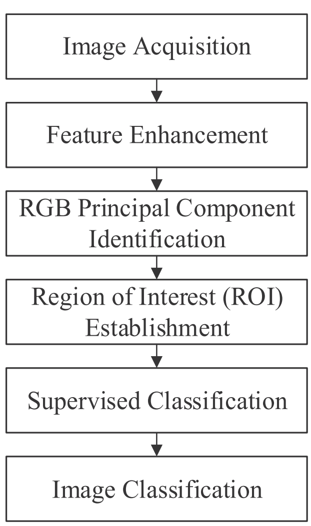

Fig. 5. Flowchart of the geospatial imaging technique.

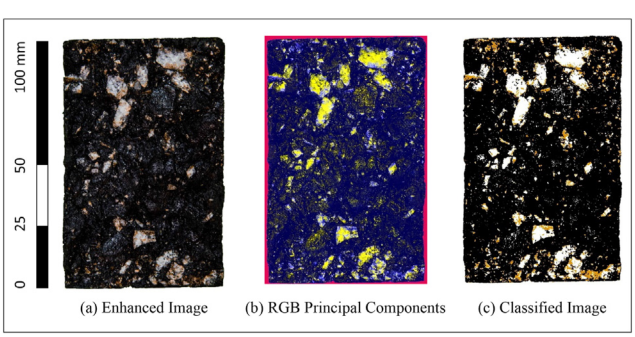

Fig. 6. Image classification with geospatial imaging technique.

findings would be further supported by the quantification of surface fracture characteristics as discussed in latter part of this paper. Other researchers found that mixtures within certain RAP content threshold would result in equal or higher ITS, else a decline would occur [22,26–27].

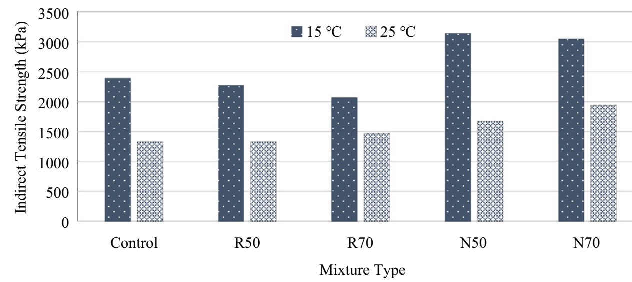

Fig. 7. ITS of asphalt mixtures at 15℃ and 25℃.

Table 6
Tukey's range test for ITS at 15℃ and 25℃.

Mixture Type	15℃	25℃
Control	B	A
R50	A, B	A
R70	A	A, B
N50	C	B
N70	C	C

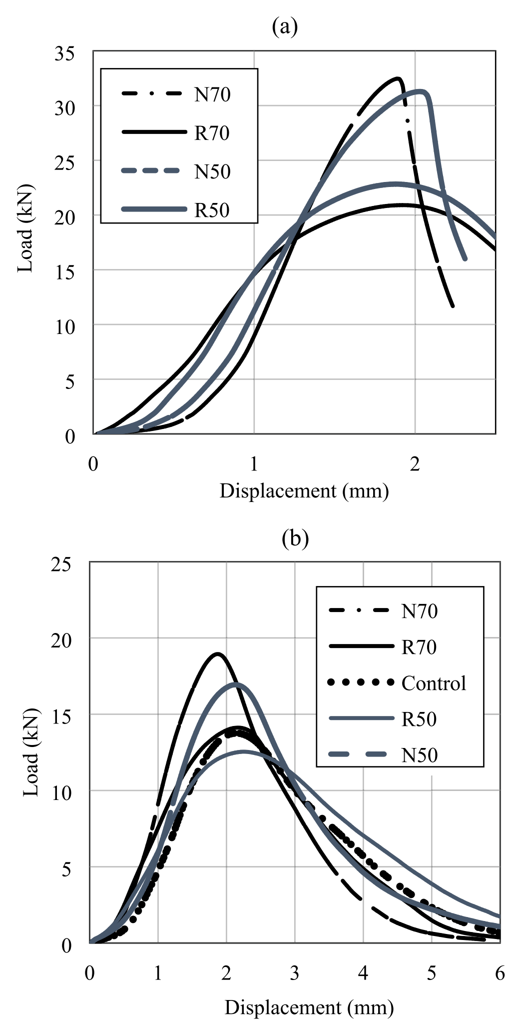

Fig. 8. Typical load–displacement curves of ITS tests at 15℃ and 25℃: (a) 15℃ and (b) 25℃.

3.2. Fracture toughness

Fracture toughness is often evaluated with the simulation of a vertical reflective crack. However, interesting observations reported by previous study suggest that a combination of vertical and sliding displacement was more likely to occur when the pavement was loaded by a moving vehicle [15–16]. This would result in an angled-crack. In this study, the digital image correlation technique enabled these fracture modes to be visualised clearly as shown in Fig. 9. The configured notch position successfully resulted in a tensile-shear fracture as the crack propagated at an angle towards the applied load initially before the formation of a vertical crack.This assessment approach presents a unique load–displacement curve to study the RAP mixtures' fracture mechanics. The computed pre-peak slopes from these load–displacement curves are presented in Fig. 10, while Fig. 11 and Table 7 compare the fracture energy. When weakened by an artificial notch, the pre-peak slopes gave an indication of the mortar flexibility during crack propagation. Steep slope indicates that the mixture has low mortar flexibility but it may not necessarily result in low fracture energy. Therefore, both fracture energy and pre-peak slope were computed to characterise the fracture toughness of the mixtures. For instance, steep slope with low fracture energy as observed in N70 mixture implied that the mixture exhibited brittle characteristics.

In general, tensile-shear induced fractures yield higher fracture energy than pure tensile fracture. The contrast between fracture energy of RAP mixtures in mode I and mixed-mode I/II fractures was apparent when compared with the control mixture. The control mixtures demonstrated versatile and consistent performance when subjected to the identical evaluation. As such, fracture

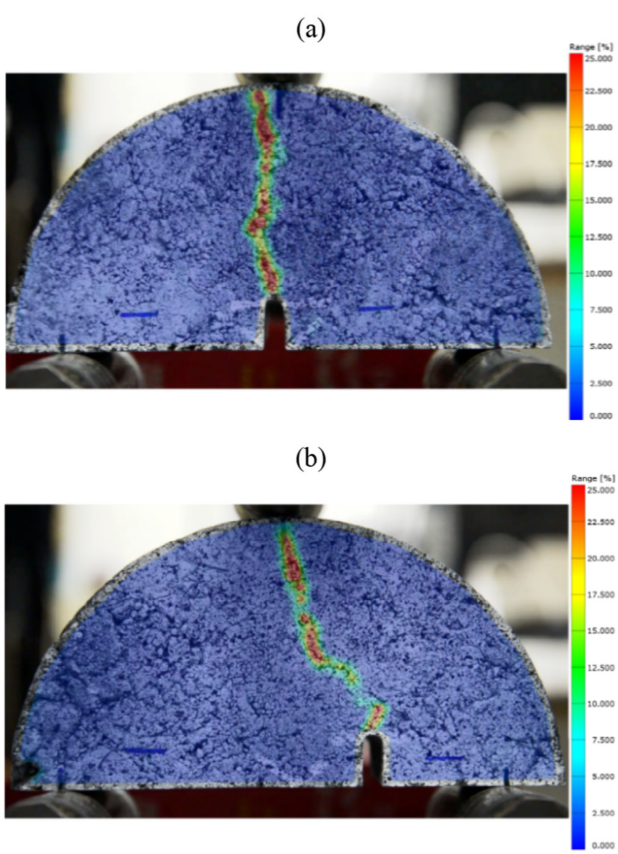

Fig. 9. Fracture simulations visualised with digital image correlation technique: (a) mode I and (b) mixed-mode I/II.

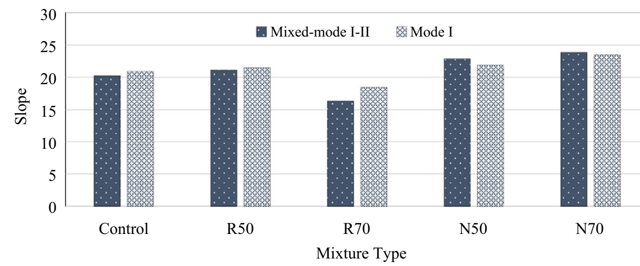

Fig. 10. Pre-peak slope of load–displacement curves.

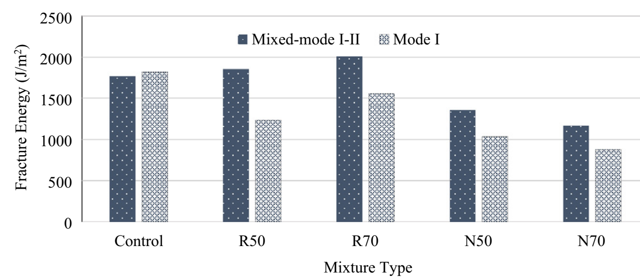

Fig. 11. Mode I and mixed-mode I/II fracture energy of the asphalt mixtures.

Table 7
Tukey's range test for fracture energy.

Mixture Type	Mode I	Mixed-mode I/II
Control	A	A, B
R50	B	A, B
R70	A	A
N50	B, C	A, B
N70	C	B

energy registered in fracturing control mixture with both modes varied marginally. Meanwhile, brittle material with low mortar flexibility such as N50 and N70 mixtures constituted low fracture energy. Unlike N50 and N70 mixtures, the R50 and R70 mixtures showed promising performance when the mixtures experienced a tensile-shear fracture especially for R70 mixture. Nonetheless, the relative improvement in resisting mode I fracture was unapparent for R50 mixture.

To be specific, the reduction in fracture toughness of non-rejuvenated RAP mixtures was attributed to the mixtures' quasi-brittle characteristics, where narrow and sharp curves were developed as shown in Fig. 12(b). A typical compliant curve was developed from fracturing the control mixture as shown in Fig. 12(a). Unlike the compliant curve shown in Fig. 12(a), curve pattern in Fig. 12(b) shared identical characteristics with those generated by conventional dense mix asphalt cracked at very low temperature as outlined by Artamendi and Khalid [28]. This implies that the non-rejuvenated mixture was stiffer than the virgin mixture. The strain tolerance prior to the occurrence of macro-crack was minimal. An acute drop beyond the peak also shows that the formation of macro-crack was instantaneous. As a result, non-rejuvenated mixtures were considerably weaker than virgin mixtures in terms of fracture toughness.

Fig. 13 compares the typical load–displacement curves with quasi-brittle and softened characteristics. What stands out in Fig. 13(b) is the softening curve exhibited by the rejuvenated mixture when experiencing tensile-shear fracture, resulting in a more gradual pre-peak slope and larger area under the curves. The load spikes shown in Fig. 13(a) clearly indicated that the non-rejuvenated mixture's ability in resisting shear was comparatively

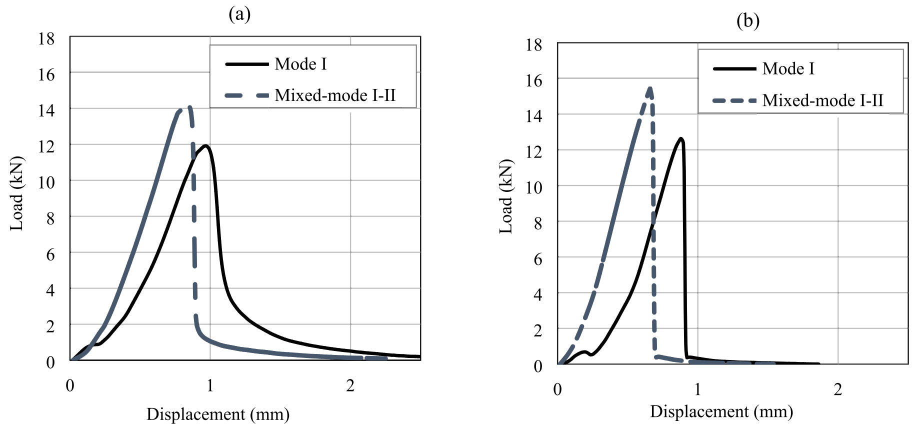

Fig. 12. Typical load–displacement curves with compliant and quasi-brittle characteristics: (a) compliant curves, Control and (b) quasi-brittle curves, N70.

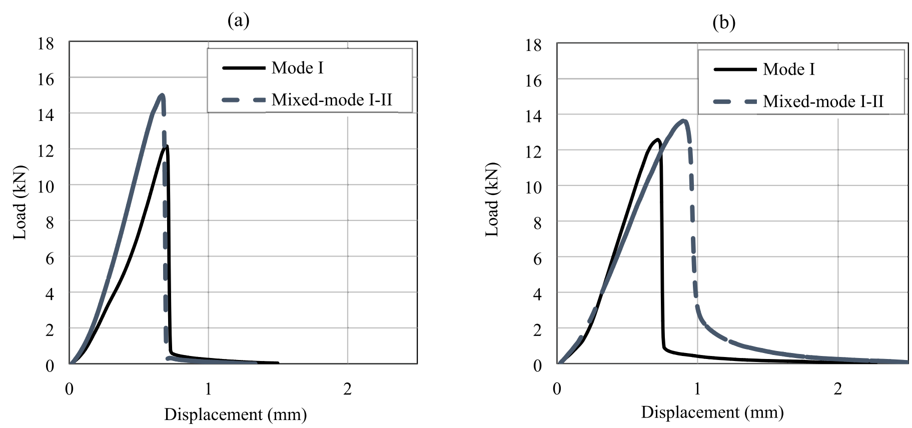

Fig. 13. Typical load–displacement curves with quasi-brittle and softened characteristics: (a) quasi-brittle curves, N50 and (b) softened curves, R50.

weak. Similar finding was reported in previous research on 50% RAP with rejuvenator [29].

Comparing the rejuvenated mixtures' load–displacement curves offered yet another noteworthy finding. Contrary with the previous trends, rejuvenated mixture with higher RAP content, R70 exhibited a distinctly softened curves when compared with R50 mixture. As shown in Fig. 14, the typical curve characteristics indicated that more work was required to fracture R70 mixture in tensile-shear mode. The softening effects of rejuvenation have skewed the peak of the compliant curve away from peak load of mode I curve. Thus, crack propagation induced by shear damage was delayed to a significant extent with the development of a more gradual slope, resulting in a broader area under the curve.

A higher rejuvenator mass used in R70 mixture to rejuvenate more RAP content may be accounted for such behaviour. Another possible explanation may be attributed to the composite behaviour of asphalt material. Mixing 70% virgin material with 30% RAP content was known to produce a highly coherent mixture with enhanced mechanical performance [1]. Likewise, inversely proportional mixture composition where RAP material was dominant may also reproduce such mechanical properties with the aid of rejuvenator. The mixture would behave homogeneously and exhibit the characteristics of the predominant material. In this case, the rejuvenated material is the predominant material of the mixture as it incorporates a very high proportion of similar materials.

3.3. Fracture surface characteristics

With the use of geospatial software, the surface damage characteristics caused by fracture can be quantified and compared digitally. Through careful interpretation, it was found that the natural selection of crack path would always adhere to the least cost path principle, where fracture would take place via the weakest plane of the mixture. These weak planes were attributed to the mixture's mechanical properties under the influence of material behaviours in different conditions. For a well-mixed virgin mixture with high quality aggregates, asphalt mortar would naturally form the weakest plane when subjected to fracture in a warm environment. In other words, a comparatively high proportion of cohesive damage would transpire in place of adhesive and aggregate damages as the softened mortar layer was said to have the least cost (smallest friction factor or hindrance) for a fracture path.

In this study, the comprehension of the least cost path principle is the key to interpret the fracture surface characteristics quantified by the geospatial software. The typical post-processed fracture surfaces of 100-mm diameter ITS test specimens at 25℃ and 15℃ are presented in Figs. 15 and 16, respectively.

Even through mere visual inspection, it was possible to confirm that cohesive damage was dominant for virgin and rejuvenated mixtures at warm condition, while adhesive and aggregate damages were apparent for non-rejuvenated mixtures at both temperatures. Furthermore, it was found that the aggregate damage was comparatively significant at lower temperature when comparison

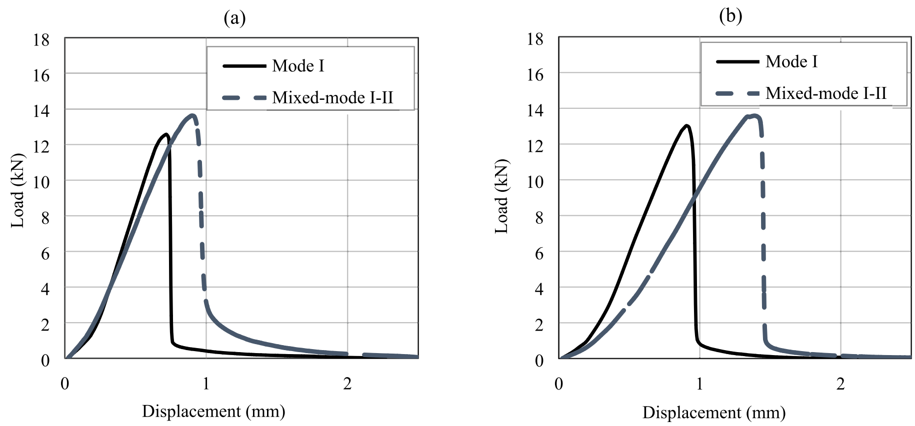

Fig. 14. Typical load–displacement curves with marginally softened and distinctly softened characteristics: (a) marginally softened curves, R50 and (b) distinctly softened curves, R70.

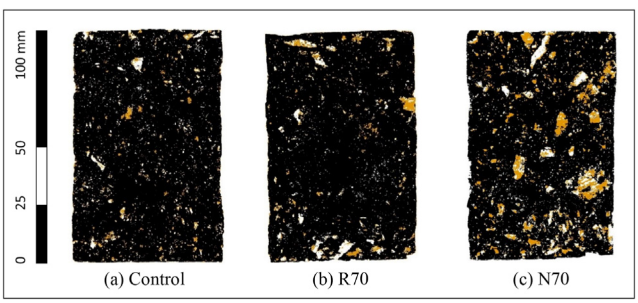

Fig. 15. Post-processed fracture surfaces of ITS test specimens at 25℃.

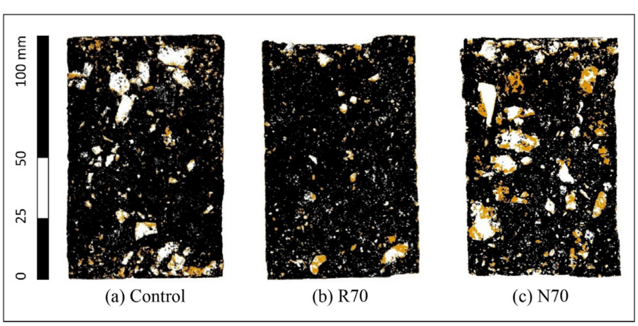

Fig. 16. Post-processed fracture surfaces of ITS test specimens at 15℃.

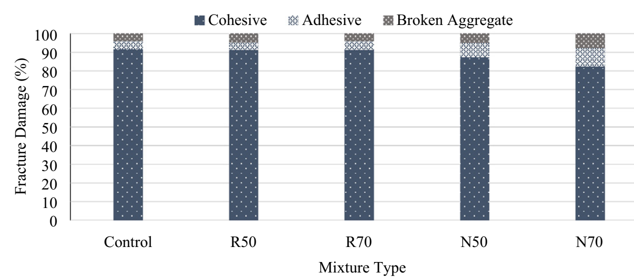

Fig. 17. Fracture damage characteristics of ITS test at 25℃.

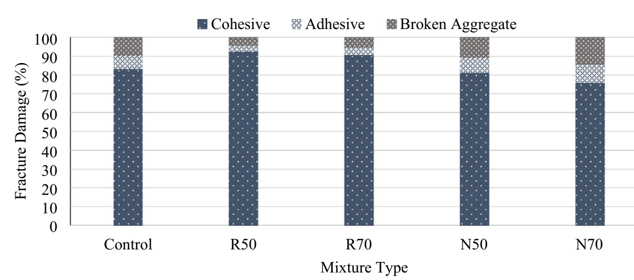

Fig. 18. Fracture damage characteristics of ITS test at 15℃.

was made within single mixture type between Figs. 15 and 16. The trends were in line with the findings from the Indirect Tensile Strength test.

To ensure unambiguous comparison, the geospatial software allowed damage characteristics to be represented numerically and compared statistically. Graphical representation of these results are presented in Figs. 17 and 18. In additions, Tukey's range test was carried out to compare these fracture properties and results are tabulated in Tables 8 and 9.

Several observations could be drawn from these results. Firstly, the softening effects of the rejuvenator were found to be statistically significant. In terms of cohesive damage, the rejuvenated mixtures performed comparably with virgin mixtures at warm condition. The mortar layer was sufficiently softened that the fracture would bypass the aggregate by meandering through the soft mortar layer instead of a direct path, resulting in more cohesive

Table 8
Tukey's range test for fracture surface characteristics of ITS test at 25℃.

Mixture Type	Cohesive	Adhesive	Broken Aggregate
Control	A	A	A
R50	A	A	A
R70	A	A	A, B
N50	B	B	A, B
N70	C	B	B

Table 9
Tukey's range test for fracture surface characteristics of ITS test at 15℃.

Mixture Type	Cohesive	Adhesive	Broken Aggregate
Control	B, C	B, C	A, B
R50	A	A	A
R70	A, B	A, B	A
N50	C	C	A
N70	C	C	B

damage. On the other hand, the mortar layer stiffened when evaluated at lower temperature. This resulted in higher aggregate damage for all mixtures as it was more economical to fracture through the aggregate via shorter crack path. Cohesive damage in rejuvenated mixtures only varied slightly than the results in warm condition. On the contrary, the percentage in broken aggregates for virgin mixture increased significantly when compared with rejuvenated mixtures at this temperature, indicating stiffer mortar. Other non-rejuvenated mixtures also resulted in even higher percentage of broken aggregates due to the combination of weak RAP aggregates and stiff mortar. Therefore, the mortar stiffness with respect to mixture type could potentially be graded through this systematic comparison.

For a non-rejuvenated mixture, other modes of fracture damage took precedence as the mortar layer was no longer the weakest plane in relative terms. Typical RAP aggregates tend to be poorly coated or partially coated before mixing with virgin binder [11]. Acting as an inhomogeneous composition, fracture may tend to take place between the contact surfaces of the aged and virgin mortar layers in non-rejuvenated mixtures. The fracture would then propagate along the weak plane towards the small contact surfaces between virgin mortar and RAP aggregates, resulting in stripping. In other words, the high percentage of adhesive damage could be an indication of poor blending between RAP and virgin materials. On that account, non-rejuvenated RAP mixtures mixed at low temperatures would result in higher adhesive damage but the low adhesive damage of rejuvenated mixtures indicate that the RAP-virgin materials were comparatively well mixed.

Fig. 19 depicts the damage characteristics induced by pure tensile fracture in notched SCB fracture test. Despite its apparent resemblance with fracture surfaces of ITS test specimen fractured at 15℃, there was no strong trend in terms of percentage of broken aggregates. The lack of strong trend was likely to be caused by the short fracture path between the notch and the position of applied load. The contributing factor to this observation was crack distance. Crack distance is one of the vital parameters in the least cost path principle. At a low temperature and short distance, crack would not meander through the weak mortar layer but rather through the aggregates due to the increase in mortar stiffness at low temperature. Therefore, the fracture path of asphalt mixture was highly dependent on the stiffness of the asphalt mortar and aggregate mechanical strength at specific temperature. The tensile-shear damage characteristics of SCB fracture test specimens is shown in Fig. 20. Overall, an increase in adhesive damage was observed for all specimens owing to the effects of shear. However, rejuvenated RAP mixtures exhibit lower adhesive damage. Without rejuvenator, aggregate-mortar stripping is an issue for RAP mixtures with very high RAP content such as N70 mixture.

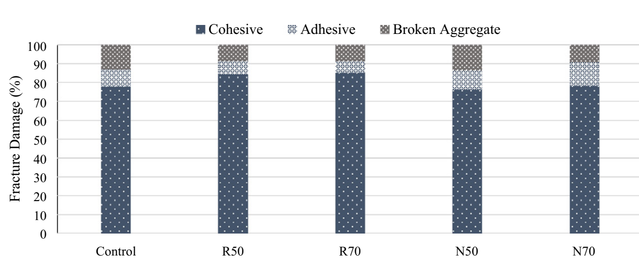

Fig. 19. Fracture damage characteristics of mode I SCB fracture test at 10℃.

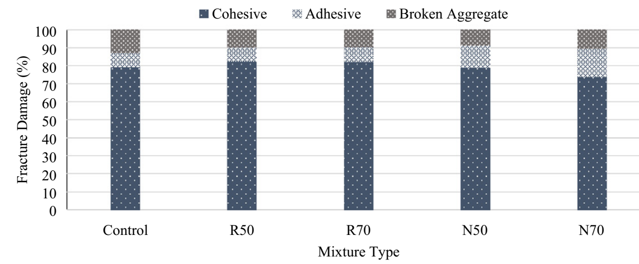

Fig. 20. Fracture damage characteristics of mixed-mode I/II SCB fracture test at 10℃.

4. Conclusion

Through the combination of conventional and innovative approaches, the following conclusions can be drawn:

- When rejuvenated, the RAP mixtures performed comparably with virgin mixtures in terms of ITS. Rejuvenated mixtures and non-rejuvenated mixtures with higher RAP content performed slightly poorer at lower temperature than their respective counterpart. Hence, it could be inferred that at warm condition, the mixture rupture was highly stiffness-dependent, while aggregate strength played a bigger role at low temperature.
- Tensile-shear fracture simulation was made possible with an offset notch configuration. The digital image correlations technique allowed the fracture path to be visualised clearly. Visual observation showed that the crack propagated at an angle towards the applied load initially before the formation of a vertical crack.
- Notched SCB test, indicated that the R70 mixture outperformed other mixtures when subjected to tensile-shear fracture. A distinctly softened curve and marginally softened curves were observed in the load–displacement graphs of R70 and R50 mixtures, respectively. Non-rejuvenated mixtures showcased quasi-brittle characteristics during the SCB test, resulting in steeper pre-peak slope and lower fracture energy in general.
- Quantification of fracture properties from ITS and notched SCB fracture using geospatial imaging technique showed that cohesive damage was dominant in mixtures with softer mortar layer, while aggregate damage was apparent when stiff mortar layer was present during the fracture. Adhesive damage was particularly apparent in non-rejuvenated mixtures due to poor degree of blending between RAP and virgin materials. Fracture path seemed to adhere to the least cost path principle and governed by mortar stiffness when investigated in terms of fracture surface characteristics. This supported the trends in ITS test.

CRediT authorship contribution statement

J.K. Ong: Methodology, Formal analysis, Investigation, Writing - original draft. **L. Gungat:** Conceptualization, Investigation, Writing - review & editing, Visualization. **M.O. Hamzah:** Conceptualization, Visualization, Supervision, Funding acquisition.

Declaration of Competing Interest

The authors declare that they have no known competing financial interests or personal relationships that could have appeared to influence the work reported in this paper.

Acknowledgement

The authors would like to acknowledge the Universiti Sains Malaysia that has funded this research grant through the Research University Individual Grant Scheme (RUI Grant Number 1001/PAWAM/814231) which enables this paper to be written.

References

[1] Copeland, A. (2011), Reclaimed Asphalt Pavement in Asphalt Mixtures: State of the Practice, Report No. FHWA-HRT-11-021, Federal Highway Administration, McLean, Virginia
[2] M. Zaumanis, R.B. Mallick, R. Frank, 100% Recycled Hot Mix Asphalt: A Review and Analysis, Resour. Conserv. Recycl. 92 (2014) 230–245.
[3] Holtz, K. and Eighmy, T. T. (2000), Scanning European Advances in The Use of Recycled Materials in Highway Construction, AASHTO Quarterly Magazine, Vol. 78, No.3, American Association of State Highway and Transportation Officials, Northwest, Washington, D.C.
[4] K.R. Hansen, A. Copeland, Asphalt Pavement Industry Survey on Recycled Materials and Warm-Mix Asphalt Usage: 2016, 7th Annual Asphalt Pavement Industry Survey, IS 138(7e), National Asphalt Pavement Association, Lanham, Maryland, 2017.
[5] EAPA, European Asphalt Pavement Association, Asphalt in Figures 2016, Version 22-1-2018, Belgium, Brussels, 2018.
[6] Wayman, M., Nicholls, C., Mollenhauer, K., Mcnally, C., Tabaković, A., Gibney, A., Varveri, A., Cassidy, S., Shahmohammadi, R. and Gilbert, K. (2012), Re-road - End-of-life Strategies of Asphalt Pavements: Delieverable 3.4, Life Cycle Assessment of Reclaimed Asphalt, 7th Framework Programme, European Commision DG Research, European Union.
[7] Al-Qadi, I. L., Aurangzeb, Q., Carpenter, S. H., Pine, W. J. and Trepanier, J. (2012), Impact of High RAP Content on Structural and Performance Properties of Asphalt Mixtures, Report No. FHWA-ICT-12-002, Illinois Center for Transportation, University of Illinois at Urbana-Champaign, Urbana, Illinois
[8] M. Zaumanis, R.B. Mallick, L. Poulikakos, R. Frank, Influence of Six Rejuvenators on the Performance Properties of Reclaimed Asphalt Pavement (RAP) Binder and 100% Recycled Asphalt Mixtures, Constr. Build. Mater. 71 (2014) 538–550.
[9] P. Kriz, D.L. Grant, B.A. Veloza, M.J. Gale, A.G. Blahey, J.H. Brownie, R.D. Shirts, S. Maccarrone, Blending and Diffusion of Reclaimed Asphalt Pavement and Virgin Asphalt Binders, Road Materials and Pavement Design 15 (1) (2014) 78–112.
[10] B. Huang, G. Li, D. Vukosavljevic, X. Shu, B. Egan, Laboratory Investigation of Mixing Hot-mix Asphalt with Reclaimed Asphalt Pavement, Transportation Research Record: Journal of the Transportation Research Board 1929 (2005) 37–45.
[11] E.N. Johnson, R.C. Olson, Best Practices for RAP Use Based on Field Performance, Report No. MN/RC 2009–15, Minnesota Department of Transportation, Minnesota, Maplewood, 2009.
[12] M.O. Hamzah, M.R. Kakar, S.A. Quadri, J. Valentin, Quantification of Moisture Sensitivity of Warm Mix Asphalt Using Image Analysis Technique, J. Cleaner Prod. 68 (2014) 200–208.
[13] M.R. Kakar, M.O. Hamzah, J. Valentin, Analyzing the Stripping Potential of Warm Mix Asphalt Using Imaging Technique Vol. 236, No (2017) 1.
[14] S.R. Omranian, M.O. Hamzah, T.S. Yee, M.R. Mohd Hasan, Effects of Short-term Ageing Scenarios on Asphalt Mixtures' Fracture Properties Using Imaging Technique and Response Surface Method, Int. J. Pavement Eng. (2018) 1–19.
[15] L. Sun, J. Ren, S. Zhang, Fracture Characteristics of Asphalt Concrete in Mixed-Loading Mode at Low-Temperature Based on Discrete-Element Method, J. Mater. Civ. Eng. 30 (12) (2018) 04018321.
[16] M. Ameri, A. Mansourian, M.H. Khavas, M. Aliha, M.R. Ayatollahi, Cracked Asphalt Pavement under Traffic Loading – A 3D Finite Element Analysis, Eng. Fract. Mech. 78 (8) (2011) 1817–1826.
[17] J. Shen, S. Amirkhanian, J. Aune Miller, Effects of Rejuvenating Agents on Superpave Mixtures Containing Reclaimed Asphalt Pavement, J. Mater. Civ. Eng. 19 (5) (2007) 376–384.
[18] PWD, Standard Specification For Road Works, Section 4: Flexible Pavement, JKR/SPJ/2008-S4, Malaysian Public Works Department, Kuala Lumpur, Wilayah Persekutuan Kuala Lumpur, 2008.
[19] L. Gungat, N.I.M. Yusoff, M.O. Hamzah, Effects of RH-WMA Additive on Rheological Properties of High Amount Reclaimed Asphalt Binders, Constr. Build. Mater. 114 (2016) 665–672.
[20] Van Weezenbeek Specialties, Testing Report for the Performance of Prephalt FBK, Van Weezenbeek Specialties, Heerhugowaard, North Holland, 2017.
[21] M.O. Hamzah, L. Gungat, B. Golchin, Estimation of Optimum Binder Content of Recycled Asphalt Incorporating a Wax Warm Additive Using Response Surface Method, Int. J. Pavement Eng. 18 (8) (2017) 682–692.
[22] H. Shao, L. Sun, L. Liu, Z. You, X. Yang, A Novel Double-drum Mixing Technique for Plant Hot Mix Asphalt Recycling with High Reclaimed Asphalt Pavement Content and Rejuvenator, Constr. Build. Mater. 134 (2017) 236–244.
[23] ASTM, ASTM D6931–17: Standard Test Method for Indirect Tensile Test (ITS) Strength of Asphalt Mixtures, American Society for Testing and Materials International, West Conshohocken, Pennsylvania, 2017.
[24] AASHTO, AASHTO TP 124: Standard Method of Test for Determining the Fracture Potential of Asphalt Mixtures Using Semicircular Bend Geometry (SCB) at Intermediate Temperature, American Association of State Highway and Transportation Officials, Northwest, Washington, D.C., 2015.
[25] M. Ameri, A. Mansourian, S. Pirmohammad, M.R.M. Aliha, M.R. Ayatollahi, Mixed Mode Fracture Resistance of Asphalt Concrete Mixtures, Eng. Fract. Mech. 93 (2012) 153–167.
[26] B.J. Putman, F. Xiao, Investigation of Warm Mix Asphalt (WMA) Technologies and Increased Percentages of Reclaimed Asphalt Pavement (RAP) in Asphalt Mixtures, Report No. FHWA-SC-12-05, Glenn Department of Civil Engineering, Clemson University, Clemson, South Carolina, 2012.
[27] James Richard Willis, Mihai Marasteanu (Eds.), Improved Mix Design, Evaluation, and Materials Management Practices for Hot Mix Asphalt with High Reclaimed Asphalt Pavement Content, Transportation Research Board, Washington, D.C., 2013.
[28] I. Artamendi, H.A. Khalid, A Comparison between Beam and Semi-circular Bending Fracture Tests for Asphalt, Road Materials and Pavement Design 7 (1) (2011) 163–180.
[29] W. Song, B. Huang, X. Shu, Influence of Warm-mix Asphalt Technology and Rejuvenator on Performance of Asphalt Mixtures Containing 50% Reclaimed Asphalt Pavement, J. Cleaner Prod. 192 (2018) 191–198.